Physical Mechanism of Grain Refinement in Solidification of Undercooled Melts

M. Schwarz,[1] A. Karma,[2] K. Eckler,[1] and D. M. Herlach[1]

[1]*Institut für Raumsimulation, Deutsche Forschungsanstalt für Luft-und Raumfahrt, D-51140 Köln, Germany*

[2]*Physics Department, Northeastern University, Boston, Massachusetts 02115*

(Received 21 April 1994)

It is proposed that the widely observed transitions in solidification of undercooled melts from a coarse grained dendritic to a grain refined equiaxed microstructure result from the fragmentation of dendrites by remelting during the period following recalescence where the interdendritic melt solidifies. This mechanism is supported by the experimental demonstration in Cu-Ni alloys that the transition undercoolings vary with cooling rate in a way which is relatively well described quantitatively by a simple fragmentation model. The latter also predicts the occurrence to two transitions, both of which are observed.

PACS numbers: 61.50.Cj, 64.70.Dv, 68.45.–v

Recently, essential progress has been made in the analysis of rapid solidification phenomena and their consequences to the formation of novel metastable phases and microstructures [1,2]. On one hand, laser resolidification experiments have been intensely used to study the formation of metastable supersaturated phases from the liquid state which are now well described by solute-trapping models [3]. On the other hand, undercooling experiments have demonstrated that rapid solidification is achieved even at slow cooling rates and, correspondingly, leads to deviations from local equilibrium at the solidification front [4,5]. In parallel, new theoretical models have improved our understanding of the nonequilibrium processes occurring during rapid solidification [1,2].

An important outcome of high undercooling experiments has been the observation of a largely unexpected "grain refined equiaxed microstructure." If the undercooling exceeds a critical value ΔT^* the microstructure is found to change abruptly within an undercooling interval of a few degrees from a classic coarse grained dendritic microstructure—such as that typically observed at very low undercooling—to a grain refined equiaxed microstructure. Since the first detection of such a transition by Walker in undercooled Ni melts [6], this grain refinement process has been observed in a great variety of different metallic systems [7,8]. This indicates that the grain refinement transition is a rather universal process occurring in undercooled melts. However, a unique description of the physical origin of this process has remained lacking up until now [9]. The purpose of this Letter is to pinpoint its origin.

A model is introduced in which the transition between microstructures is assumed to result from dendrite fragmentation by remelting. In conjunction, an experimental study of dendrite growth behavior and microstructural changes as a function of undercooling is performed on a $Ni_{70}Cu_{30}$ alloy. This alloy is chosen for the investigations since it is a solid solution whose thermodynamic properties are well known. As in many other alloys [7], the measurements reveal the existence of two consecutive microstructural transitions with increasing undercooling. As shown in Fig. 1, a grain refined equiaxed microstructure is observed at smaller undercoolings ($\Delta T < \Delta T_1^*$), a coarse grained dendritic microstructure at intermediate undercoolings ($\Delta T_1^* < \Delta T < \Delta T_2^*$), and a reentrance of the grain refined equiaxed microstructure at larger undercoolings ($\Delta T > \Delta T_2^*$).

The alloys were prepared from constituents of purity better than 99.99% by *in situ* melting in a rf-levitation coil under high-purity environment into spheres of about 6 mm diameter. Undercooling conditions were established in an electromagnetic levitation apparatus under high-purity environmental conditions. The experimental setup allows high undercoolings owing to the avoidance of container-wall-induced nucleation. Crystallization of the undercooled melt was externally initiated by triggering the melt with a stimulus needle at a well defined undercooling. The temperature during heating and cooling was recorded by a two color pyrometer with an absolute accu-

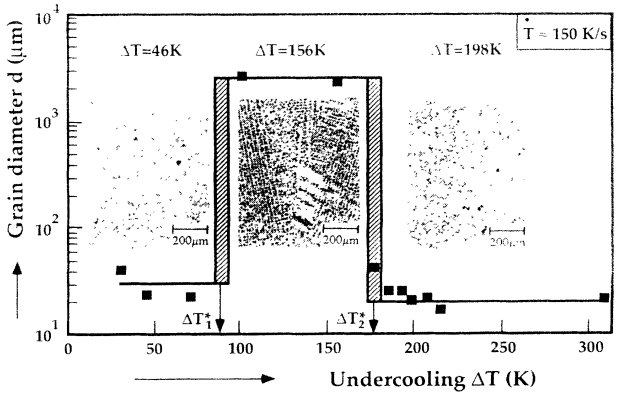

FIG. 1. Grain diameter d as a function of undercooling ΔT. ΔT_1^* and ΔT_2^* denote the undercoolings of transition between microstructures. The insets exhibit micrographs of samples undercooled by different amounts.

0031-9007/94/73(10)/1380(4)$06.00

racy of ± 3 K. Further details of the experimental setup are given elsewhere [10].

Figure 2 shows a typical temperature-time profile. During heating the sample melts in the interval between T_l (liquidus temperature) and T_s (solidus temperature) marked by a change in the slope of the temperature-time trace. After a moderate overheating the sample is cooled and undercooled to a temperature T_n at which nucleation is triggered. Crystallization then sets in, leading to a rapid temperature rise during recalescence which is due to the release of heat of fusion. During recalescence, solidification takes place under quasiadiabatic conditions. Dendrites are formed at the nucleation point and propagate rapidly through the volume of the melt. Nonequilibrium effects at the tip are important during this process. Once the temperature has reached a temperature between T_l and T_s, the remaining interdendritic melt solidifies during a "plateau phase" under quasistationary equilibrium conditions at the solid-liquid interface. The plateau duration Δt_{pl} is exclusively controlled by the heat transfer from the sample to the environment. It is essentially an experimental control parameter which can be directly measured and, importantly for the present investigation, can be varied by changing the cooling rate. After all the liquid is solidified, the sample cools down to ambient temperature. The undercooling ΔT and the plateau duration are directly inferred from the temperature-time profile. The microstructure of the as-solidified samples were investigated by conventional optical metallography (Fig. 1).

For the analysis of the experimental results, we assume that the refinement of the microstructure is caused by remelting and coarsening of primary formed dendrites. This assumption is supported by the observation that the average grain diameter is comparable to the dendrite trunk radius which, in turn, is comparable to the dendrite sidebranch spacing. Furthermore, the transitional microstructures indicate the presence of spherelike particles in the wake of a dendritic microstructure. This observation suggests that these spherelike elements originate from the breakup of primary dendrites and their sidebranches by remelting. Physically, this process is driven by surface tension: the system attempts to minimize its surface area via heat and solute diffusion in the bulk phases. Dendrite breakup requires a characteristic time, $\Delta t_{\mathrm{bu}}(\Delta T)$, which depends on the undercooling. According to this picture, one should observe a grain refined equiaxed microstructure if $\Delta t_{\mathrm{bu}} < \Delta t_{\mathrm{pl}}$, in which breakup occurs before the sample has had time to completely solidify, and a coarse grained dendritic microstructure if $\Delta t_{\mathrm{bu}} > \Delta t_{\mathrm{pl}}$. This implies that the undercoolings of transition between the two microstructures are determined by the relation

$$\Delta t_{\mathrm{bu}}(\Delta T^*) \approx \Delta t_{\mathrm{pl}} . \tag{1}$$

The problem of determining ΔT^* is now reduced to calculating the breakup time. A first principle calculation of this time represents a virtually impossible task, even with the current computational means. We therefore use a simple model in which the dendrite trunk is stripped of its branches and treated as an infinitely long isolated solid cylinder imbedded in a uniform liquid of temperature T_l and composition c_0 equal to the nominal composition of the alloy. This model obviously represents a very crude geometrical approximation of an actual trunk but contains the correct surface tension driving force for fragmentation. It is easy to show that such an idealized cylindrical trunk will break up into an array of quasispherical particles due to a shape instability similar to that of rodlike eutectic composites [11]. The classic Rayleigh instability of a liquid stream is a direct hydrodynamic analog of this process. Consider a small cylindrically symmetric perturbation of the dendrite trunk of the form

$$r(z,t) = R + \delta_k \exp[ikz + \omega(k;R)\,t] + \text{c.c.},$$

which is spatially periodic along the central z axis of the trunk; $r(z,t)$ denotes the perpendicular distance of the solid-liquid interface to the z axis, R the unperturbed trunk radius, δ_k the amplitude of the perturbation, and $\omega(k;R)$ its amplification rate. A straightforward linear stability analysis yields the expression for dilute alloys [12],

$$\omega(k;R) = \frac{d_0 D_T}{R^3} f_1(kR) \times \left[\frac{1}{f_2(kR)} - \frac{m_l c_0 (1 - k_E)}{\Delta H_f / C_p} \frac{D_T}{D_C} \right]^{-1}, \tag{2}$$

where D_T denotes the thermal diffusivity taken to be equal in both planes, D_c the solute diffusivity in the liquid, m_l the equilibrium liquidus slope, k_E the equilibrium partition coefficient, ΔH_f the heat of fusion, C_p the specific heat at constant pressure, $d_0 = \Gamma C_p / \Delta H_f$ the capillary length, and Γ the Gibbs-Thomson coefficient. We have defined

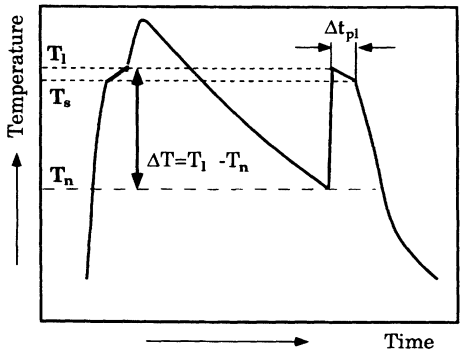

FIG. 2. Schematic temperature-time (T-t) profile obtained from an undercooling experiment using electromagnetic levitation. The undercooling, $\Delta T = T_l - T_n$, and the plateau duration, δT_{pl}, are directly inferred from experimental profiles.

the functions $f_1(kr) \equiv kR[1 - (kR)^2]K_1(kR)/K_0(kR)$ and $f_2(kR) = 1 + K_0(kR)I_1(kR)/[I_0(kR)K_1(kR)]$, where K_0, K_1, I_0, and I_1 denote the standard modified Bessel functions. The breakup time is assumed to be inversely proportional to the amplification rate of the fastest growing perturbation of wave vector $k_{\max}$. At the level of a linear analysis, this time is also proportional to $\ln(R/\delta_{k_{\max}})$. We further assume that sidebranches perturb the trunk with an initial amplitude which scales with R, in which case this logarithmic factor becomes a constant of order unity independent of R. This yields at once the expression

$$\Delta t_{\mathrm{bu}}(\Delta T) \approx 1/\omega(k_{\max}; R(\Delta T)). \quad (3)$$

It should also be noted that the supersaturation inside the dendrite trunk resulting from solute trapping during growth provides an additional driving force for breakup (after growth) via diffusion in the solid. A crude estimate [12] indicates that this driving force is negligible at the lower undercooling transition (ΔT_1^*), where growth is too slow for trapping to be significant, and is at the very most comparable in magnitude to capillarity at the higher undercooling transition (ΔT_2^*). Hence, we suspect that the present results are not dramatically altered by the inclusion of this additional driving force. For the alloy composition investigated here, $|m_l c_0(1 - k)D_T C_p/\Delta H_f D_C| \gg 1$ (i.e., breakup is dominated by solute diffusion), in which case Eq. (3) reduces to

$$\Delta t_{\mathrm{bu}}(\Delta T) \approx \frac{3}{2}\frac{R(\Delta T)^3}{d_0 D_C}\left|\frac{m_l c_0(1 - k_E)}{\Delta H_f/C_p}\right|, \quad (4)$$

with $k_{\max}R(\Delta T) \approx 0.48$. The trunk radius is correlated to the dendrite tip radius, $R_{\mathrm{tip}}(\Delta T)$, via a proportionality constant, $z \equiv R(\Delta T)/R_{\mathrm{tip}}(\Delta T)$. This constant is determined by taking the ratio of the trunk radius, measured from micrographs of solidified samples, to the calculated tip radius at the same undercooling. When repeated for different undercoolings, this procedure yields an approximately constant value of $z \approx 20$ which was used in all our calculations. The tip radius is calculated following the exact same procedure as
ing a marginal stability criterion for the operating point of the dendrite tip [13]. This procedure offers a practical, albeit nonrigorous, substitute to using the now commonly accepted solvability theory [14] which remains difficult to carry out numerically in three dimensions. In previous studies [4,5], this procedure was found to yield reasonably accurate predictions of dendrite growth velocities over a wide range of undercoolings.

The curve $\Delta t_{\mathrm{bu}}(\Delta T)$, plotted in Fig. 3, was calculated from Eq. (4), with $R(\Delta T)$ determined as indicated above, and the numerical values given in Table I. The breakup time sharply decreases with undercooling, passes through a minimum, rises very rapidly, and finally goes through a maximum before falling down again. The occurrence of a minimum and a maximum in the $\Delta t_{\mathrm{bu}}(\Delta T)$ are linked to the dependence on tip radius. At small undercooling, dendritic growth is controlled mainly by chemical diffusion and the tip radius decreases as the concentration gradient becomes steeper. As the undercooling is further increased, solute trapping sets in, leading to a decrease of the concentration gradient and an increase of the tip radius until the absolute stability of solutal dendrites is reached. Beyond this limit, dendritic growth is purely thermally controlled and the tip radius begins to fall again due to an increase of the thermal gradient. We strongly expect that this nonmonotonic dependence of the tip radius on undercooling, which is crucial for our explanation of multiple transitions between microstructures, is a direct consequence of the aforementioned physical effects and is not an artifact of the approximate way in which this radius is calculated.

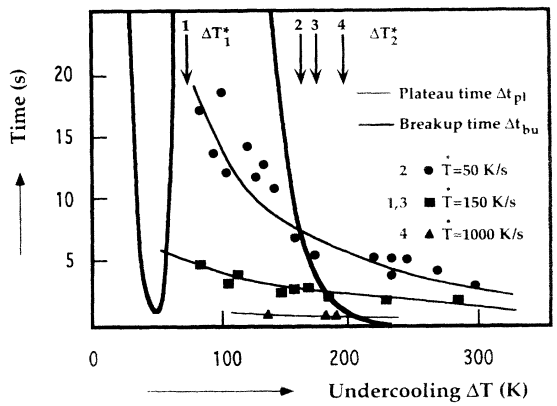

FIG. 3. Calculated dendrite breakup time vs undercooling [$\Delta t_{\mathrm{bu}}(\Delta T)$ curve and thick solid line], and measured plateau durations vs undercooling [$\Delta t_{\mathrm{pl}}(\Delta T)$ curves and thin solid lines] for three different cooling rates (see text). The arrows mark the microstructural transition temperatures as determined from the microstructure investigations of samples solidified after different undercoolings. They coincide well with the intersection points between the two curves [Eq. (1)].

TABLE I. Materials parameters of $Ni_{70}Cu_{30}$ alloy used in the calculation of the breakup time.

Parameter		Dimension	Value
Heat of fusion	ΔH_f	J/mol	1.61×10^4
Specific heat	C_p	J/(mol K)	38.3
Liquidus temperature	T_l	K	1644
Liquidus slope	m_l	K/at. %	−2.8
Diffusion coefficient	D_C	m^2/s	1.9×10^{-9}
Thermal diffusivity	D_T	m^2/s	7×10^{-6}
Partition coefficient	k_E		0.736
Gibbs-Thomson coefficient	Γ	Km	3.25×10^{-7}

The plateau durations, inferred from temperature-time profiles, are plotted in Fig. 3 as solid symbols and fitted graphically by thin solid lines which constitute the $\Delta t_{\mathrm{pl}}(\Delta T)$ curves. The three thin solid lines correspond to three series of experiments, each with a different cooling rate. The squares give the results of experiments in which the sample is cooled in the levitation coil (low cooling rate $\approx$50 K/s). The circles represent results obtained if the generator power is switched off and the sample is cooled down by being placed on a sample holder (medium cooling rate $\approx$150 K/s). Finally, the triangles give the results if the sample is quenched into a liquid metallic bath of a Ga-In-Sn alloy, which is liquid at room temperature (large cooling rate $\approx$1000 K/s) [15]. According to the predictions of the model, the intersection points between the $\Delta t_{\mathrm{bu}}(\Delta T)$ and $\Delta t_{\mathrm{pl}}(\Delta T)$ curves [Eq. (1)] define the transition undercoolings ΔT_1^* and ΔT_2^* (cf. Fig. 1). The latter should therefore depend on the plateau durations and hence on the rate at which the samples are cooled. As indicated by the arrows, which give the transition temperatures (undercoolings) determined independently from the microstructural investigations, there is an excellent quantitative agreement between the predictions of the model and the experimental findings as far as the higher critical undercoolings ΔT_2^* are concerned. The lower critical undercoolings ΔT_1^* are also in relatively good agreement despite a discrepancy of about 20 K.

In summary, we have proposed that grain refinement in undercooled melts results from a dendrite fragmentation mechanism. This is strongly supported by the fact that, when quantified in terms of a simple breakup model [12], this mechanism can (i) explain the existence of multiple transitions between microstructures, two of which are predicted and observed over the temperature range investigated, and (ii) predict the observed cooling rate dependence of the transition temperatures. The alloy concentration can be used as an additional experimental parameter to test the model since it alters the dendrite breakup time. Preliminary results of investigations in this direction confirm the conclusions of this work [16].

Three of the authors (M. S., K. H., D. M. H.) want to thank B. Feuerbacher for continuous support. Part of this work has been financially supported by the European Communities under Contract No. BE5142. The research of A. K. was supported by U.S. DOE Grant No. DE-FG02–92ER45471.

[1] W. Kurz and R. Trivedi, Acta Metall. **38**, 1 (1990).
[2] *Undercooled Metallic Melts: Properties, Solidification and Metastable Phases*, edited by D. M. Herlach, I. Egry, P. Baeri, F. Spaepen [Mater. Sci. Eng. A **178**, 1–313 (1994)].
[3] M. J. Aziz, J. Y. Tsao, M. O. Thompson, P. S. Peercy, and C. W. White, Phys. Rev. Lett. **56**, 2489 (1986).
[4] R. Willnecker, D. M. Herlach, and B. Feuerbacher, Phys. Rev. Lett. **62**, 2707 (1989).
[5] K. Eckler, R. F. Cochrane, D. M. Herlach, B. Feuerbacher, and M. Jurisch, Phys. Rev. B **45**, 5019 (1992).
[6] J. L. Walker, in *The Physical Chemistry of Process Metallurgy*, edited by G. R. St. Pierre (Interscience, New York, 1959), Pt. 2, p. 845.
[7] A. Munitz and G. J. Abbaschian, in *Undercooled Alloy Phases*, edited by E. W. Collings and C. C. Koch (AIME, Warrendale, PA, 1986), p. 23.
[8] R. Willnecker, D. M. Herlach, and B. Feuerbacher, Appl. Phys. Lett. **56**, 324 (1990).
[9] D. M. Herlach, R. F. Cochrane, I. Egry, H. J. Fecht, and A. L. Greer, Int. Mater. Rev. **38**, 273 (1993).
[10] D. M. Herlach, R. Willnecker, and F. Gillessen, in Proceedings of the 4th European Symposium on Materials Science under Microgravity [European Space Agency Report No. ESA SP-222, 1984], p. 399.
[11] H. E. Cline, Acta Metall. **19**, 481 (1971).
[12] A. Karma (to be published).
[13] J. Lipton, W. Kurz, and R. Trivedi, Acta Metall. **35**, 957 (1987); **35**, 965, (1987).
[14] For reviews, see J. S. Langer, in *Chance and Matter*, Lecture on the Theory of Pattern Formation, Proceedings of the Les Houches Summer School 1986, edited by J. Souletie, J. Vannimenus, and R. Stora (North-Holland, New York, 1987), pp. 629–711; D. Kessler, J. Koplik, and H. Levine, Adv. Phys. **37**, 255 (1988).
[15] Here, the plateau durations are determined by time-resolved measurements of the temperature change in the quenching bath using a high speed photosensing device.
[16] K. Eckler, M. Schwarz, D. M. Herlach, and A. Karma (to be published).

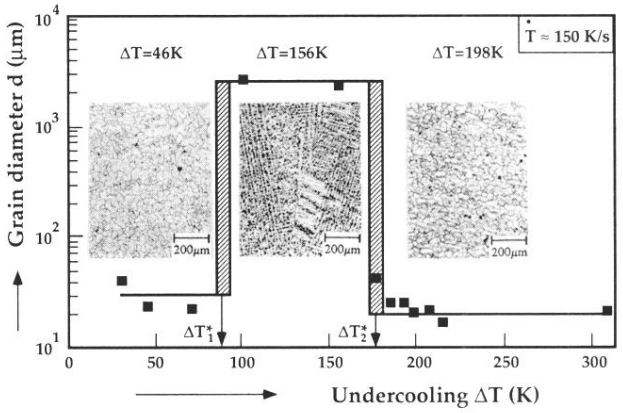

FIG. 1. Grain diameter d as a function of undercooling ΔT. ΔT_1^* and ΔT_2^* denote the undercoolings of transition between microstructures. The insets exhibit micrographs of samples undercooled by different amounts.